

Spectrally stable defect qubits with no inversion symmetry for robust spin-to-photon interface

Péter Udvarhelyi,^{1,2} Roland Nagy,³ Florian Kaiser,³ Sang-Yun Lee,⁴ Jörg Wrachtrup,³ and Adam Gali^{2,5}

¹*Department of Biological Physics, Loránd Eötvös University,
Pázmány Péter sétány 1/A, H-1117 Budapest, Hungary*

²*Wigner Research Centre for Physics, Hungarian Academy of Sciences, P.O. Box 49, H-1525 Budapest, Hungary*

³*Institute of Physics, University of Stuttgart and Institute for Quantum Science and Technology IQST, Germany*

⁴*Center for Quantum Information, Korea Institute of Science and Technology, Seoul, 02792, Republic of Korea*

⁵*Department of Atomic Physics, Budapest University of Technology and Economics, Budafoki út 8., H-1111 Budapest, Hungary*

(Dated: April 26, 2022)

Scalable spin-to-photon interfaces require quantum emitters with strong optical transition dipole moment and low coupling to phonons and stray electric fields. It is known that particularly for coupling to stray electric fields, these conditions can be simultaneously satisfied for emitters that show inversion symmetry. Here, we show that inversion symmetry is not a prerequisite criterion for a spectrally stable quantum emitter. We find that identical electron density in ground and excited states can eliminate the coupling to the stray electric fields. Further, a strong optical transition dipole moment is achieved in systems with altering sign of the ground and excited wavefunctions. We use density functional perturbation theory to investigate an optical center that lacks of inversion symmetry. Our results show that this system close to ideally satisfies the criteria for an ideal quantum emitter. Our study opens a novel rationale in seeking promising materials and point defects towards the realisation of robust spin-to-photon interfaces.

I. INTRODUCTION

Solid state defect quantum emitters are at the heart of quantum technologies. Quantum information technologies¹, quantum communication^{2,3} and nanoscale sensor applications⁴⁻⁶ require defects with long coherence times. Further, a quantum emitter with good optical properties allows for convenient optically-assisted spin state initialisation and readout^{7,8}. However, inhomogeneities in the host crystal can lead to degradation of optical properties. A predominant contribution is usually spectral diffusion and inhomogeneous broadening caused by the Stark shift effect. Optical excitation induces charge fluctuations of parasitic defects, which influence the optical properties of the investigated system^{9,10}. The quantum emitter for quantum communication technology should emit predominantly coherent photons at relatively large rate. However, especially for solid state emitters, photons are emitted either among purely electronic states (zero phonon emission) or among states with phonons being excited. Photons of the latter emission are not coherent. Therefore, the ratio of the emitted photons with zero-phonon contribution to the total emission, i.e., the Debye-Waller factor of the quantum emitter also categorizes the quality of the quantum emitter. To summarize the requirements for an ideal quantum emitter for quantum technology, it should exhibit (i) a long spin coherence time, (ii) a Debye-Waller factor close to unity, and (iii) no spectral diffusion. Deficiencies in the first criterion can be principally circumvented by dynamical decoupling schemes that can extend the coherence times further at the expense of longer measurement times¹¹, that is an inevitable technique in such host materials where no spin-free isotopes are available. On the other hand, the last criterion is, in particular, inherently bound to the defect

properties that cannot be efficiently circumvented even in optical cavities that might significantly enhance the emission in the zero-phonon-line (ZPL).

A simple solution to the problem of spectral diffusion is utilizing quantum defects with inversion symmetry that *ab ovo* do not couple to static electric stray fields¹². This condition is intimately connected to the crystal structure of the host material of the quantum emitter. This symmetry requirement excludes compound semiconductors or insulator crystals that *per se* do not host defects with inversion symmetry, although advanced production and processing technologies exist for those platforms. However, plethora of compound semiconductors or insulators are potential candidates for hosting quantum emitters, e.g., defects in silicon carbide (SiC) have favorable coherence times in naturally abundant hosts without any dynamical decoupling procedures such as neutral divacancies¹³⁻¹⁶ and negatively charged silicon-vacancies¹⁷⁻²².

In this paper, we show that the inversion symmetry is not a prerequisite criterion for a spectrally stable defect quantum emitter. We demonstrate this principle by means of density functional perturbation theory calculations on the so-called V1 center, i.e., the negatively charged silicon-vacancy at the so-called hexagonal (*h*) site in the compound semiconductor 4H silicon carbide (SiC).

II. RESULTS

A. Microscopic model of an ideal defect quantum emitter

An ideal quantum emitter should show no spectral diffusion. This property can be achieved if the electric

dipole moment remains either be zero or unchanged during the optical excitation process between the ground ($|g\rangle$) and excited ($|e\rangle$) states

$$|\langle e|\vec{r}|e\rangle|^2 - |\langle g|\vec{r}|g\rangle|^2 = 0. \quad (1)$$

On the other hand, the optical transition rate should be large

$$|\langle e|\vec{r}|g\rangle|^2 > 10 \text{ Debye}^2. \quad (2)$$

The expectation values in Eqs. (2) are generally nonzero according to the selection rules of quantum mechanics. As vector operators have $P = -1$ parity, the wavefunctions in the integral must have different parity, in order to result in a nonzero scalar.

For color centers with inversion symmetry, Eq. (1) is satisfied as the individual integrals are zero, where the wavefunctions have either gerade (even) or ungerade (odd) parity. The high optical transition rate can be achieved by large overlap between a gerade orbital and an ungerade orbital in these optical centers.

The main point of the present paper is the following statement: the inversion symmetry is not an ultimate criterion in simultaneous fulfillment of these requirements as Eq. (1) may be satisfied without the restriction that all the individual terms in Eq. (1) should be set to zero. We show below that other types of optical centers may satisfy Eq. (1).

Defects usually have axial symmetry in compound semiconductors. In this case, Eq. (1) can be satisfied for identical charge densities of the ground and excited state. In systems with axial symmetry, Eq. (2) can be separated into two parts,

$$|\langle e|\vec{r}_\perp|g\rangle|^2 + |\langle e|\vec{r}_\parallel|g\rangle|^2, \quad (3)$$

where the first contribution is typically zero for orbitally non-degenerate ground state. The second contribution can be maximized by a large overlap of the wavefunctions (already satisfied by the same density requirement), if they are well separated in their signs along the symmetry axis, i.e., alternating phase of wavefunctions. This condition restricts the optical polarization to be parallel to the symmetry axis. A possible realization of the wavefunctions that fulfills the requirements detailed above is depicted in Fig. 1 for a defect with axial (C_{3v}) symmetry.

The other requirement for an ideal quantum emitter is a high Debye-Waller factor, in order to achieve emission of coherent photons at high rate. This can be fulfilled for those defects that have negligible geometry relaxation upon optical excitation.

B. V1 center as an nearly ideal defect quantum emitter

In this paper, we identify the h -site silicon-vacancy defect (V1 center) in 4H SiC as a nearly ideal quan-

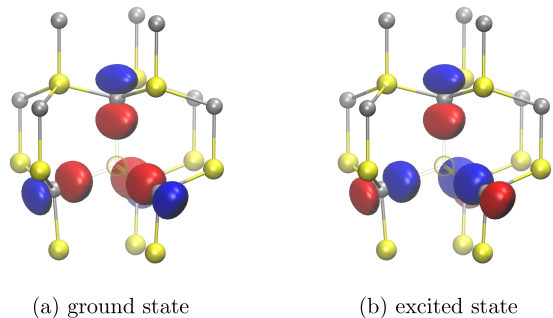


FIG. 1. Wavefunction of ideal defect quantum emitter with axial symmetry in a binary semiconductor. The different types of atoms are colored by gray and yellow balls, whereas the positive (negative) isovalues of the corresponding wavefunctions participating in the optical transition are depicted as red (blue) lobes.

TABLE I. Macroscopic electric dipole moment of the negatively charged h -site Si-vacancy defect (V1) as calculated within Berry phase approximation. ex(gr) notes the excited state electron configuration calculated with fixed ground state geometry.

transition	$\Delta p_{\text{ion}} (e\text{\AA})$	$\Delta p_{\text{el}} (e\text{\AA})$	$\Delta p_{\text{tot}} (e\text{\AA})$
gr \rightarrow ex	0	0.044	0.044
gr \rightarrow ex(gr)	0	0.039	0.039

tum emitter with no inversion symmetry. Long coherence time was already reported for this defect making it a promising candidate for spin-based quantum applications^{23,24}. In order to demonstrate that this defect also possesses all the optical requirements for quantum communication, we performed density functional (DFT) calculations and compared this defect to the negatively charged nitrogen-vacancy (NV) center in diamond that is known to exhibit a few GHz spectral diffusion even in high purity diamond samples²⁵.

The results of Berry phase evaluation for macroscopic dipole moment calculation are shown in Table I and Table II for V1 center in 4H SiC and NV center in diamond, respectively. We find that the change in the permanent dipole moments upon optical excitation for V1 center in 4H SiC is nearly 20 times smaller than that for NV center in diamond. This translates to weak coupling of optical excitation to stray electric fields for V1 center in 4H SiC, in good agreement with our very recent experimental data²⁶.

TABLE II. Macroscopic electric dipole moment of the negatively charged nitrogen-vacancy defect in diamond as calculated within Berry phase approximation.

transition	$\Delta p_{\text{ion}} (e\text{\AA})$	$\Delta p_{\text{el}} (e\text{\AA})$	$\Delta p_{\text{tot}} (e\text{\AA})$
gr \rightarrow ex	0.061	0.842	0.903

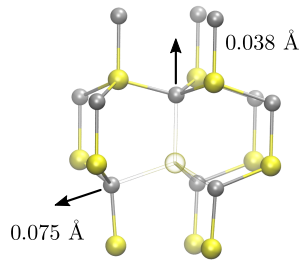


FIG. 2. Geometry relaxation of V1 center upon optical excitation. Small gray, large yellow and glass balls represent carbon, silicon atoms, and the vacant site, respectively. The movement of the first neighbor C-atoms are shown by arrows with the corresponding distances.

The geometry relaxation in the excitation transition of the V1 center is depicted in Fig. 2 which shows that the ions move outward going from the electronic ground state to the excited state. This leads to smaller than unity Debye-Waller factor in the luminescence spectrum. It is experimentally verified²⁴ to remain ~ 0.5 , which is about an order of magnitude larger than that of NV center in diamond^{3,27,28}. The second row in Table I shows the change in the dipole moments without relaxation effect at fixed ground state geometry. We conclude that the outward relaxation of ions upon optical excitation has little effect on the final difference in the dipole moments, and the change is associated with the nature of the ground state and excited state wavefunctions.

C. Origin of permanent dipole moments and strong emission from V1 center in 4H SiC

The results on the microscopic level can be interpreted by considering the electron density of defect states in the ground state. The corresponding in-gap defect levels and labels are shown in Fig. 3. This approximation neglects relaxation effects of ions and the effect of the delocalized electron bath. We approximate the origin of total change of electric dipole moment by studying the difference of electron density of these in-gap Kohn-Sham states that changes occupation during optical transition (V1 u and v levels and NV v and e levels in Fig. 3).

To visualize this scenario, we plot the electron density in the minority spin channel of the localized Kohn-Sham orbitals in the ground state (Fig. 4). NV in diamond shows a rather large change in localization and magnitude of the electron densities going from the excited state to the ground state which leads to a considerable change of electric dipole moment. However, V1 center manifests small change in localization and magnitude of the electron densities that suggests small change of electric dipole moment.

Figure 5 shows overlap of same phase for the lobe in

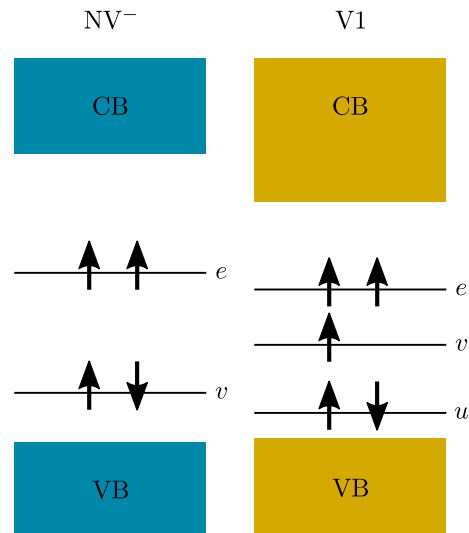


FIG. 3. Schematic visualization of ground state Kohn-Sham levels of NV and V1 center in the band gap, respectively.

axial direction resulting in a positive contribution. The basal lobes overlap with different phase resulting in negative contribution. These spatially well-separated contributions with opposite sign integrate to a rather large transition dipole moment. The calculated radiative lifetime of V1 center is 12 ns which is fairly comparable to the lifetime of NV center in diamond.

These lines of the discussion are inspired by Eqs. (1) and (2) that indeed explain well our *ab initio* results on the change of the permanent dipole moments versus the radiative lifetime.

III. DISCUSSION

Our findings have important implications in seeking materials hosting defect quantum emitters for realizing robust spin-to-photon interfaces. It is a common sense in the present literature that only defects with inversion symmetry are decoupled from stray electric fields, which significantly constrains the type of host materials. We show that the quest of inversion can be relaxed and other types of defect quantum emitters are in contention, such as V1 center in 4H SiC. In particular, 4H SiC hosts spin-active emitters, e.g., a recent study on molybdenum^{29,30}, that might have also favorable optical stability against stray electric fields. Quantum emitters in other semiconductors such as ZnO^{31,32} and GaN^{33,34} should be also revisited in this regard. Our study also provides new horizon and guidance to design novel defect quantum emitters in two-dimensional compound materials³⁵⁻³⁹ for stable spin-to-photon interface at a single photon level.

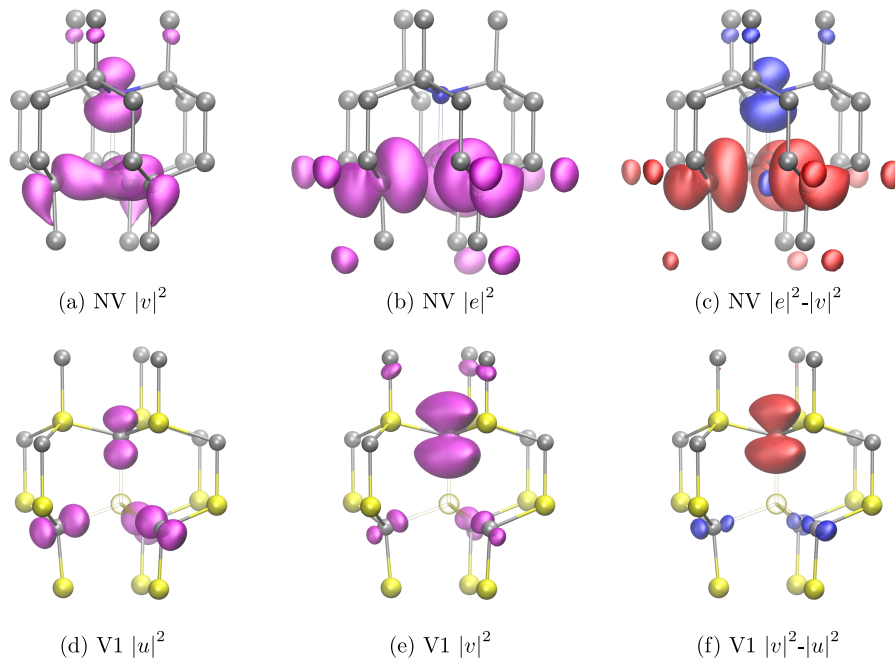


FIG. 4. Electron density isosurfaces (0.025\AA^{-3} in purple color) of the ground state in the minority spin channel for the localized Kohn-Sham states of NV center in diamond (a, b) and V1 center in 4H SiC (d, e). Their positive (negative) difference is shown in red (blue) colors in (c, f). Gray, yellow and blue balls represent carbon, silicon and nitrogen atoms, respectively. Vacancy is represented by a glass ball.

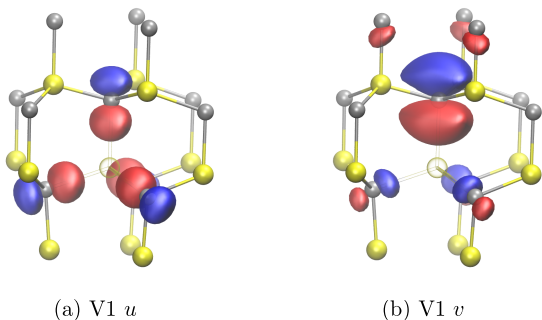


FIG. 5. Square moduli of the corresponding wavefunctions of the ground state in the minority spin channel in V1 center. The same color code is used as in Fig. 4(f).

COMPUTATIONAL DETAILS

We determined the coupling of optical excitation to the external electric fields by calculating the permanent dipole moments in the corresponding 4A_2 ground state and 4A_2 excited state of the negatively charged silicon vacancy (V1) h-site defect in 4H-SiC and the corresponding 3A ground states and 3E excited state of the negatively charged nitrogen-vacancy center in diamond using density functional theory (DFT). We also determined the radiative lifetime of V1 center in 4H SiC.

Electronic structure calculation

We applied DFT for electronic structure calculation and geometry relaxation, using the plane-wave Vienna Ab initio Simulation Package (VASP)⁴⁰⁻⁴³. The core electrons were treated in the projector augmented-wave (PAW) formalism⁴⁴. The calculations were performed with 420 eV plane wave cutoff energy and with Γ centered $2 \times 2 \times 2$ k-point mesh for the 4H SiC supercell, 420 eV plane wave cutoff energy and Γ -point for the diamond supercell, respectively. We applied spinpolarized PBE functional in these calculations⁴⁵. The model of V1 center in bulk 4H-SiC was constructed using a 432-atom hexagonal supercell whereas we used the 512-atom simple cubic supercell to model nitrogen-vacancy (NV) center in diamond. The excited state electronic structure and geometry were calculated by constraint occupation of states, or Δ SCF method⁴⁶.

Permanent dipole moment calculation

We calculated the permanent dipole moments in the ground and excited state. The difference in the dipole moments is associated with the coupling parameter of the electric fields and the optical transition. To calculate the permanent dipole moments of the corresponding states, we used the VASP implementation of both Born effective charge calculation using density functional per-

turbation theory⁴⁷ and the Berry phase theory of polarization^{48–50}. In a DFT calculation, one can define the change in macroscopic electronic polarization (P) as an adiabatic change in the Kohn-Sham potential (V_{KS})

$$\frac{\partial \mathbf{P}}{\partial \lambda} = -\frac{if e \hbar}{\Omega m_e} \sum_{\mathbf{k}} \sum_{n=1}^M \sum_{m=M+1}^{\infty} \frac{\langle \psi_{\mathbf{k}n}^{(\lambda)} | \hat{\mathbf{p}} | \psi_{\mathbf{k}m}^{(\lambda)} \rangle \langle \psi_{\mathbf{k}m}^{(\lambda)} | \frac{\partial V_{KS}}{\partial \lambda} | \psi_{\mathbf{k}n}^{(\lambda)} \rangle}{(\epsilon_{\mathbf{k}n}^{(\lambda)} - \epsilon_{\mathbf{k}m}^{(\lambda)})^2} + c.c., \quad (4)$$

where f is the occupation number, e elemental charge, m_e electron mass, Ω cell volume, M number of occupied bands, \vec{p} momentum operator. The first part of the equation corresponds to the electronic part of the permanent dipole moment (p_{el}) whereas the second part corresponds to the contribution of ions (p_{ion}) to the permanent dipole moment. In a periodic gauge, where the wavefunctions are cell-periodic and periodic in the reciprocal space, the permanent dipole moment takes a form similar to the Berry phase expression

$$\Delta \mathbf{P} = \frac{ife}{8\pi^3} \sum_{n=1}^M \int_{BZ} d\mathbf{k} \langle u_{\mathbf{k}n} | \nabla_{\mathbf{k}} | u_{\mathbf{k}n} \rangle. \quad (5)$$

Using density functional perturbation theory (DFPT), $\nabla_{\mathbf{k}} | u_{\mathbf{k}n} \rangle$ can be calculated from the Sternheimer equations with similar self-consistent iterations as in the self-consistent field DFT

$$(\mathbf{H}_{\mathbf{k}} - \epsilon_{\mathbf{k}n} \mathbf{S}_{\mathbf{k}}) \nabla_{\mathbf{k}} | u_{\mathbf{k}n} \rangle = -\frac{\partial (\mathbf{H}_{\mathbf{k}} - \epsilon_{\mathbf{k}n} \mathbf{S}_{\mathbf{k}})}{\partial \mathbf{k}} | u_{\mathbf{k}n} \rangle. \quad (6)$$

Radiative lifetime calculation

We determined the radiative transition rate between the ground and excited 4A_2 states by calculating the energy dependent dielectric function $\epsilon_r(E)$. The spontaneous transition rate is given by the Einstein coefficient

$$A = \frac{n\omega^3 |\mu|^2}{3\pi\epsilon_0 \hbar c^3}, \quad (7)$$

where n is the refractive index, $\hbar\omega$ is the transition energy, μ is the optical transition dipole moment, ϵ_0 is the vacuum permittivity, c is the speed of light. μ is proportional to the integrated imaginary dielectric function (I) of the given transition

$$|\mu|^2 = \frac{\epsilon_0 V}{\pi} \int \text{Im} \epsilon_r(E) dE = \frac{\epsilon_0 V I}{\pi}, \quad (8)$$

where V is the volume of the supercell. Thus, the radiative lifetime can be given by

$$\tau_r = \frac{3\pi^2 \hbar c^3}{n\omega^3 V I}. \quad (9)$$

In our particular implementation, we applied the following procedure and parameters. We fit a Lorentzian function to the first peak of $\text{Im} \epsilon_r(E)$. The results are $I = 0.389$ eV and $\hbar\omega = 1.387$ eV. Using the refractive index $n = 2.6473$ of 4H SiC and the cell volume of $V = 4.5346$ nm³, the radiative lifetime can be calculated using Eq. (9).

ACKNOWLEDGMENT

The support from National Research, Development and Innovation Office in Hungary (NKFIH) Grant Nos. 2017-1.2.1-NKP-2017-00001 (National Quantum Technology Program) and NVKP_16-1-2016-0043 (NVKP Program) as well as Grant No. NN127902 (EU QuantERA Nanospin consortial project) and from the EU Commission (Asteriqs project) is acknowledged.

COMPETING INTERESTS

There is no competing interests.

AUTHOR CONTRIBUTION

P. U. carried out the calculations and participated in writing the paper. F. K., R. N., S.-Y. L., and J. W. participated in the discussion of the results and contributed in writing the paper. A. G. conceived and managed this research, and wrote the paper.

¹ B. E. Kane, Nature **393**, 133 EP (1998), article.

² E. Togan, Y. Chu, A. S. Trifonov, L. Jiang, J. Maze, L. Childress, M. V. G. Dutt, A. S. Sørensen, P. R. Hemmer, A. S. Zibrov, and M. D. Lukin, Nature **466**, 730 EP (2010).

³ M. Atatüre, D. Englund, N. Vamivakas, S.-Y. Lee, and J. Wrachtrup, Nature Reviews Materials **3**, 38 (2018).

⁴ C. L. Degen, F. Reinhard, and P. Cappellaro, Rev. Mod. Phys. **89**, 035002 (2017).

⁵ F. Casola, T. van der Sar, and A. Yacoby, Nature Reviews Materials **3**, 17088 EP (2018), review Article.

⁶ M. Niethammer, M. Widmann, S.-Y. Lee, P. Stenberg, O. Kordina, T. Ohshima, N. T. Son, E. Janzén, and J. Wrachtrup, Phys. Rev. Applied **6**, 034001 (2016).

⁷ L. Robledo, L. Childress, H. Bernien, B. Hensen, P. F. A. Alkemade, and R. Hanson, Nature **477**, 574 EP (2011).

⁸ L. J. Rogers, K. D. Jahnke, M. H. Metsch, A. Sipahigil, J. M. Binder, T. Teraji, H. Sumiya, J. Isoya, M. D. Lukin, P. Hemmer, and F. Jelezko, Phys. Rev. Lett. **113**, 263602

- (2014).
- ⁹ H. D. Robinson and B. B. Goldberg, *Phys. Rev. B* **61**, R5086 (2000).
 - ¹⁰ L. C. Bassett, F. J. Heremans, C. G. Yale, B. B. Buckley, and D. D. Awschalom, *Phys. Rev. Lett.* **107**, 266403 (2011).
 - ¹¹ D. D. Awschalom, R. Hanson, J. Wrachtrup, and B. B. Zhou, *Nature Photonics* **12**, 516 (2018).
 - ¹² A. Sipahigil, K. D. Jahnke, L. J. Rogers, T. Teraji, J. Isoya, A. S. Zibrov, F. Jelezko, and M. D. Lukin, *Phys. Rev. Lett.* **113**, 113602 (2014).
 - ¹³ N. T. Son, P. Carlsson, J. ul Hassan, E. Janzén, T. Umeda, J. Isoya, A. Gali, M. Bockstedte, N. Morishita, T. Ohshima, and H. Itoh, *Phys. Rev. Lett.* **96**, 055501 (2006).
 - ¹⁴ W. F. Koehl, B. B. Buckley, F. J. Heremans, G. Calusine, and D. D. Awschalom, *Nature* **479**, 84 EP (2011).
 - ¹⁵ A. L. Falk, B. B. Buckley, G. Calusine, W. F. Koehl, V. V. Dobrovitski, A. Politi, C. A. Zorman, P. X. L. Feng, and D. D. Awschalom, *Nature Communications* **4**, 1819 EP (2013), article.
 - ¹⁶ D. J. Christle, P. V. Klimov, C. F. de las Casas, K. Szász, V. Ivády, V. Jokubavicius, J. Ul Hassan, M. Syväjärvi, W. F. Koehl, T. Ohshima, N. T. Son, E. Janzén, A. Gali, and D. D. Awschalom, *Phys. Rev. X* **7**, 021046 (2017).
 - ¹⁷ N. Mizuochi, S. Yamasaki, H. Takizawa, N. Morishita, T. Ohshima, H. Itoh, and J. Isoya, *Phys. Rev. B* **66**, 235202 (2002).
 - ¹⁸ D. Riedel, F. Fuchs, H. Kraus, S. Váth, A. Sperlich, V. Dyakonov, A. A. Soltamova, P. G. Baranov, V. A. Ilyin, and G. V. Astakhov, *Phys. Rev. Lett.* **109**, 226402 (2012).
 - ¹⁹ H. Kraus, V. A. Soltamov, D. Riedel, S. Váth, F. Fuchs, A. Sperlich, P. G. Baranov, V. Dyakonov, and G. V. Astakhov, *Nature Physics* **10**, 157 EP (2013), article.
 - ²⁰ H. Kraus, V. A. Soltamov, F. Fuchs, D. Simin, A. Sperlich, P. G. Baranov, G. V. Astakhov, and V. Dyakonov, *Scientific Reports* **4**, 5303 EP (2014), article.
 - ²¹ O. O. Soykal, P. Dev, and S. E. Economou, *Phys. Rev. B* **93**, 081207 (2016).
 - ²² M. Widmann, S.-Y. Lee, T. Rendler, N. T. Son, H. Fedder, S. Paik, L.-P. Yang, N. Zhao, S. Yang, I. Booker, A. Denisenko, M. Jamali, S. A. Momenzadeh, I. Gerhardt, T. Ohshima, A. Gali, E. Janzén, and J. Wrachtrup, *Nat Mater* **14**, 164 (2015).
 - ²³ D. Simin, H. Kraus, A. Sperlich, T. Ohshima, G. V. Astakhov, and V. Dyakonov, *Phys. Rev. B* **95**, 161201 (2017).
 - ²⁴ R. Nagy, M. Widmann, M. Niethammer, D. B. R. Dasari, I. Gerhardt, O. O. Soykal, M. Radulaski, T. Ohshima, J. Vučković, N. T. Son, I. G. Ivanov, S. E. Economou, C. Bonato, S.-Y. Lee, and J. Wrachtrup, *Phys. Rev. Applied* **9**, 034022 (2018).
 - ²⁵ P. Siyushev, H. Pinto, M. Vörös, A. Gali, F. Jelezko, and J. Wrachtrup, *Phys. Rev. Lett.* **110**, 167402 (2013).
 - ²⁶ R. Nagy, M. Niethammer, M. Widmann, Y.-C. Chen, P. Udvarhelyi, C. Bonato, J. U. Hassan, R. Karhu, I. G. Ivanov, N. T. Son, J. R. Maze, T. Ohshima, O. O. Soykal, A. Gali, S.-Y. Lee, F. Kaiser, and J. Wrachtrup, (2018).
 - ²⁷ A. Alkauskas, B. B. Buckley, D. D. Awschalom, and C. G. V. de Walle, *New Journal of Physics* **16**, 073026 (2014).
 - ²⁸ G. m. H. Thiering and A. Gali, *Phys. Rev. B* **96**, 081115 (2017).
 - ²⁹ A. Csóré, A. Gällström, E. Janzén, and A. Gali, *Materials Science Forum* **858**, 261 (2016).
 - ³⁰ T. Bosma, G. J. J. Lof, C. M. Gilardoni, O. V. Zwier, F. Hendriks, B. Magnusson, A. Ellison, A. Gällström, I. G. Ivanov, N. T. Son, R. W. A. Havenith, and C. H. v. d. Wal, *npj Quantum Information* **4**, 48 (2018).
 - ³¹ A. J. Morfa, B. C. Gibson, M. Karg, T. J. Karle, A. D. Greentree, P. Mulvaney, and S. Tomljenovic-Hanic, *Nano Letters* **12**, 949 (2012), pMID: 22248087, <https://doi.org/10.1021/nl204010e>.
 - ³² O. Neitzke, A. Morfa, J. Wolters, A. W. Schell, G. Kewes, and O. Benson, *Nano Letters* **15**, 3024 (2015), pMID: 25816112, <https://doi.org/10.1021/nl504941q>.
 - ³³ A. M. Berhane, K.-Y. Jeong, Z. Bodrog, S. Fiedler, T. Schröder, N. V. Triviño, T. Palacios, A. Gali, M. Toth, D. Englund, and I. Aharonovich, *Advanced Materials* **29**, 1605092 (2017).
 - ³⁴ Y. Zhou, Z. Wang, A. Rasmita, S. Kim, A. Berhane, Z. Bodrog, G. Adamo, A. Gali, I. Aharonovich, and W.-b. Gao, *Science Advances* **4**, eaar3580 (2018).
 - ³⁵ T. T. Tran, K. Bray, M. J. Ford, M. Toth, and I. Aharonovich, *Nat Nano* **11**, 37 (2016).
 - ³⁶ S. Tongay, J. Suh, C. Ataca, W. Fan, A. Luce, J. S. Kang, J. Liu, C. Ko, R. Raghunathanan, J. Zhou, F. Ogletree, J. Li, J. C. Grossman, and J. Wu, *Scientific Reports* **3**, 2657 EP (2013), article.
 - ³⁷ N. Saigal and S. Ghosh, *Applied Physics Letters* **109**, 122105 (2016), <https://doi.org/10.1063/1.4963133>.
 - ³⁸ Y.-M. He, G. Clark, J. R. Schaibley, Y. He, M.-C. Chen, Y.-J. Wei, X. Ding, Q. Zhang, W. Yao, X. Xu, C.-Y. Lu, and J.-W. Pan, *Nature Nanotechnology* **10**, 497 EP (2015).
 - ³⁹ A. Srivastava, M. Sidler, A. V. Allain, D. S. Lembke, A. Kis, and A. Imamoglu, *Nature Nanotechnology* **10**, 491 EP (2015).
 - ⁴⁰ G. Kresse and J. Hafner, *Phys. Rev. B* **47**, 558 (1993).
 - ⁴¹ G. Kresse and J. Furthmüller, *Phys. Rev. B* **54**, 11169 (1996).
 - ⁴² G. Kresse and J. Furthmüller, *Computational Materials Science* **6**, 15 (1996).
 - ⁴³ J. Paier, M. Marsman, K. Hummer, G. Kresse, I. C. Gerber, and J. G. Ángyán, *The Journal of Chemical Physics* **124**, 154709 (2006).
 - ⁴⁴ P. E. Blöchl, *Phys. Rev. B* **50**, 17953 (1994).
 - ⁴⁵ J. P. Perdew, K. Burke, and M. Ernzerhof, *Phys. Rev. Lett.* **77**, 3865 (1996).
 - ⁴⁶ A. Gali, E. Janzén, P. Deák, G. Kresse, and E. Kaxiras, *Phys. Rev. Lett.* **103**, 186404 (2009).
 - ⁴⁷ M. Gajdoš, K. Hummer, G. Kresse, J. Furthmüller, and F. Bechstedt, *Phys. Rev. B* **73**, 045112 (2006).
 - ⁴⁸ R. D. King-Smith and D. Vanderbilt, *Phys. Rev. B* **47**, 1651 (1993).
 - ⁴⁹ D. Vanderbilt and R. D. King-Smith, *Phys. Rev. B* **48**, 4442 (1993).
 - ⁵⁰ R. Resta, *Rev. Mod. Phys.* **66**, 899 (1994).